ATR-FTIR characterization of organic functional groups and inorganic ions in ambient aerosols at a rural site

Charity Coury, Ann M. Dillner*

University of California Davis, Crocker Nuclear Laboratory, One Shields Ave., Davis, CA 95616, USA

ARTICLE INFO

ABSTRACT

An Attenuated Total Reflectance-Fourier Transform Infrared (ATR-FTIR) spectroscopic method was used to measure organic functional groups and inorganic ions at Tonto National Monument (TNM), an Interagency Monitoring of Protected Visual Environments (IMPROVE) sampling site in a rural area near Phoenix, Arizona. Functional groups and ions from common aerosol compound classes such as aliphatic and aromatic CH, methylene, methyl, aldehydes/ketones, carboxylic acids, ammonium sulfate and nitrate as well as functional groups from difficult to measure compound classes such as esters/lactones, acid anhydrides, carbohydrate hydroxyl and ethers, amino acids, and amines were quantified. On average, ~33% of the PM$_{1.0}$ mass was composed of organic aerosol. The average (standard deviation) composition of the organic aerosol at TNM was 34% (6%) biogenic functional groups, 21% (5%) oxygenated functional groups, 28% (7%) aliphatic hydrocarbon functional groups (aliphatic CH, methylene and methyl) and 17% (1%) aromatic hydrocarbon functional groups. Compositional analysis, functional group correlations, and back trajectories were used to identify three types of events with source signatures: primary biogenic-influenced, urban-influenced, and regional background. The biogenic-influenced event had high concentrations of amino acids and carbohydrate hydroxyl and ether, as well as aliphatic CH and aromatic CH functional groups and qualitatively high levels of silicate. The urban-influenced events had back trajectories traveling directly from the Phoenix area and high concentrations of hydrocarbons, oxygenated functional groups, and inorganic ions. This aerosol characterization suggests that both primary emissions in Phoenix and secondary formation of aerosols from Phoenix emissions had a major impact on the aerosol composition and concentration at TNM. The regional background source had low concentrations of all functional groups, but had higher concentrations of biogenic functional groups than the urban source.

© 2008 Elsevier Ltd. All rights reserved.

1. Introduction

Atmospheric aerosols contribute to radiative forcing, adverse health effects, adverse environmental effects, and visibility degradation (Jacobson et al., 2000). In order to understand and mitigate the impacts of atmospheric aerosols, it is important to determine their physical and chemical properties as well as their sources. This information is difficult to determine for the carbonaceous component of aerosols due to its wide range of sources, complex nature and collection and analysis challenges.

Carbonaceous aerosol sources are very diverse, including gas and particulate phase emissions, anthropogenic and biogenic emissions, as well as complex secondary formation in the atmosphere. Quantification of organic aerosols is a difficult task because there are hundreds to thousands of organic compounds in the atmosphere. The most widely used organic aerosol analysis methods are thermal optical methods, which quantify the elemental carbon and organic carbon (OC) in the aerosol, but not the organic mass (OM). Gas chromatography/mass spectrometry (GC/MS) is used to quantify organic compounds on a molecular level. This method is well established for identifying specific tracer compounds that can be used to determine the contribution of specific sources to the ambient aerosol, but can identify only a fraction of the organic mass in ambient aerosol (Rogge et al., 1993; Pio et al., 2001). GC/MS requires a relatively large amount of aerosol mass, an extraction step, different columns or complex derivatization procedures to detect compounds of varying polarity, and cannot detect very large molecules (Yu et al., 1998). In order to bridge the gap between thermal optical methods and GC/MS, we developed a method (Coury and Dillner, 2008) utilizing attenuated total reflectance Fourier transform infrared (ATR-FTIR) spectroscopy that identifies and quantifies the functional groups in all of the

* Corresponding author. Tel.: +1 530 752 1124.
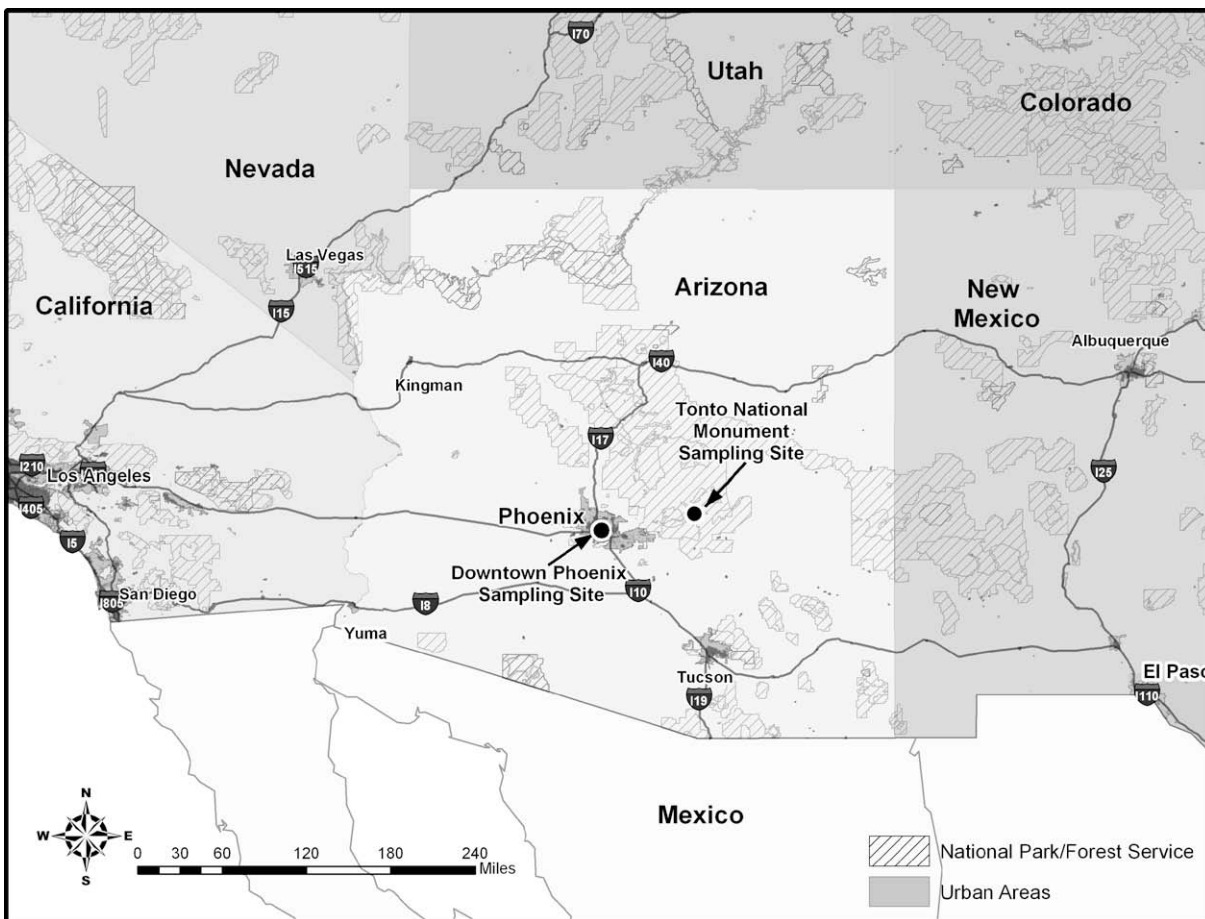 *E-mail address:* amdillner@ucdavis.edu (A.M. Dillner).

Fig. 1. Location of Tonto National Monument and Phoenix, Arizona sampling sites.

organic mass, requires only small sample sizes and no sample preparation. The method is ideally suited for characterizing the organic fraction in Class I regions (National Parks and Wilderness Areas) where concentrations are typically lower than urban areas.

The visibility in Class I areas is protected by the 1977 Clean Air Act Amendments (CAA). Interagency Monitoring of Protected Visual Environments (IMPROVE, http://vista.cira.colostate.edu/improve/) was created in 1985 to measure aerosol composition at Class I area in order to monitor the progress towards the goals set forth in the CAA. Air quality in the Superstition Wilderness a Class I area in the Sonoran Desert, is monitored at the Tonto National Monument (TNM) IMPROVE site. This site is of special interest due to its proximity to a large urban area, metropolitan Phoenix. Previously, we presented results of clustered back trajectory analysis and historical particulate matter concentrations (collected and analyzed by the IMPROVE network) at TNM (Coury and Dillner, 2007). The back trajectories showed significant flow patterns over the Phoenix urban area, especially during summer months. This analysis allowed us to attribute inorganic ion and soil elements to sources or source regions. However, when the analysis was performed on organic carbon data, the results provided little information on the sources of this aerosol component, indicating the need for more detailed analysis of the carbon fraction. The goal of this study is to characterize the OM aerosol fraction in size segregated samples at Tonto National Monument, using the ATR-FTIR method described in Coury and Dillner (2008), and use the measured functional groups and inorganic ions to determine the extent to which different sources and source regions impact OM concentrations at the site.

2. Experimental methods

2.1. Sampling

Particulate matter sampling was conducted at the Tonto National Monument (TNM) IMPROVE sampling site, which is located in the northeast corner of the Superstition Wilderness, approximately 60 miles east of Phoenix (Fig. 1). Size segregated, physical and chemical measurements of aerosols were made at TNM in winter (January) and summer (June and July) 2004. TNM experienced low relative humidity, little or no cloud cover and only one day of rain (the last day of winter sampling) during the winter and summer sampling.

In order to gain some insight into the composition of particulate upwind of TNM and the impact of organic carbon emissions in Phoenix on TNM, size segregated particulate samples were collected in Phoenix (Fig. 1) during winter (two days at the end of January and beginning of February) and summer (three days in August) 2004. Sampling in Phoenix was conducted at the Phoenix IMPROVE site which is in a residential neighborhood 4 miles north of the city center. Because there are a limited number of samples collected in Phoenix and they were not collected simultaneously with the TNM samples, it cannot be assumed that the air parcels arriving at TNM from Phoenix on sample have the same aerosol composition as the Phoenix samples. However, the Phoenix samples were taken during both winter and summer on days with low relative humidity, little or no cloud cover and no rain very similar to the conditions during the TNM sampling. The Phoenix samples therefore provide only an estimate of the particulate

composition in Phoenix during the TNM sampling. Additional sampling was conducted at an urban-fringe site, Goldfield, located between TNM and Phoenix. However, the atmospheric conditions were considerably different on the sampling days at Goldfield, compared to the other sites, so the data is only used in a qualitative way (Fig. 2).

At all sites, twenty-four hour samples (midnight to midnight) for ATR-FTIR analysis were collected using a 10-stage micro-orifice uniform deposit impactor (MOUDI, MSP Corp. model 110, Marple et al., 1991) on 47 mm diameter Teflon substrates (Teflo, 1 μm pore size, Pall Life Sciences, Ann Harbor, MI). At TNM, parallel samples were obtained with one MOUDI using Teflon substrates to measure gravimetric mass and inorganic ions using ion chromatography (Mulik et al., 1976) and another MOUDI using aluminum foil substrates for organic and elemental carbon analysis. The OC data were routinely below the measurement detection limit so the data could not be used. Substrates from the five impactor stages which collected particles with aerodynamic diameter (D_a) between 0.056 and 1.0 μm were analyzed. A 20 in. curved stainless steel tube was connected to each of the MOUDI inlets to prevent large particles and precipitation from entering the samplers. The MOUDIs were operated at a nominal flow rate of 30 l min^{-1} and flows were measured (using a BIOS DryCal DC 2 flowmeter) before and after each sampling event and average flows were used in concentration calculations.

2.2. FTIR analyses

Samples were analyzed according to procedures in Coury and Dillner (2008). Briefly, MOUDI samples were analyzed on a Thermo Nicolet IR 300 FTIR spectrometer operated with a deuterated triglycine sulfate (DTGS) detector and equipped with a Foundation Series horizontal attenuated total reflectance (ATR) accessory at the sampling site or nearby within 10 h after acquisition. Teflon substrates were removed from the sampler and placed directly onto the ATR crystal to obtain sample spectra for wavelengths between

4000 and 700 cm^{-1} with 2 cm^{-1} resolution by averaging 120 scans. A blank Teflon filter spectrum was collected each day to monitor instrument drift. Between each sample spectrum acquisition, the ATR ZnSe crystal was cleaned with isopropanol, and an air background spectrum was obtained to ensure that the crystal was completely clean.

Ambient spectra were used to identify compound classes present in the aerosol (Coury and Dillner, 2008). Representative ambient infrared spectra from the three sampling sites, Phoenix, Goldfield and TNM with particle $D_a = 0.32$–0.56 μm are shown in Fig. 2. These spectra show many overlapping spectral features, which result in shoulders and broad peaks, much like previously reported ambient spectra (e.g. Blando et al., 1998; Maria et al., 2003). As shown in Fig. 2, the prominent spectral features are from ammonium sulfate and nitrate (3300–3000, 1430, 1385, and 1110 cm^{-1}), carbonyl groups (1800–1600 cm^{-1}), aliphatic and aromatic C–H (denoted Al–CH and Ar–CH) (3100–2700 cm^{-1}), hydroxyl groups (3600–3300 cm^{-1}) and carbon–oxygen bonds at 1070 cm^{-1}.

The FTIR system was calibrated using multi-component calibration standards and a multivariate algorithm (Coury and Dillner, 2008). These methods were chosen to accurately identify and quantify functional groups in aerosol samples which produce overlapping and complex spectra. Mixtures of many compounds in each compound class identified in the ambient spectra (Table S1 in Coury and Dillner, 2008) were used to create laboratory standards. Calibration standards were made by drying various known masses of the laboratory standards directly onto the ATR crystal and covering the crystal with a Teflon filter before spectra acquisition. The compound classes used in the calibration were decomposed into functional groups. IR spectroscopy of complex mixtures can quantify concentrations of functional groups not compound classes. Table 1 lists the atoms included in each functional group. Each functional group represents only the atoms listed in the table, not the complete molecule. For example, the concentration of the carboxylic acid
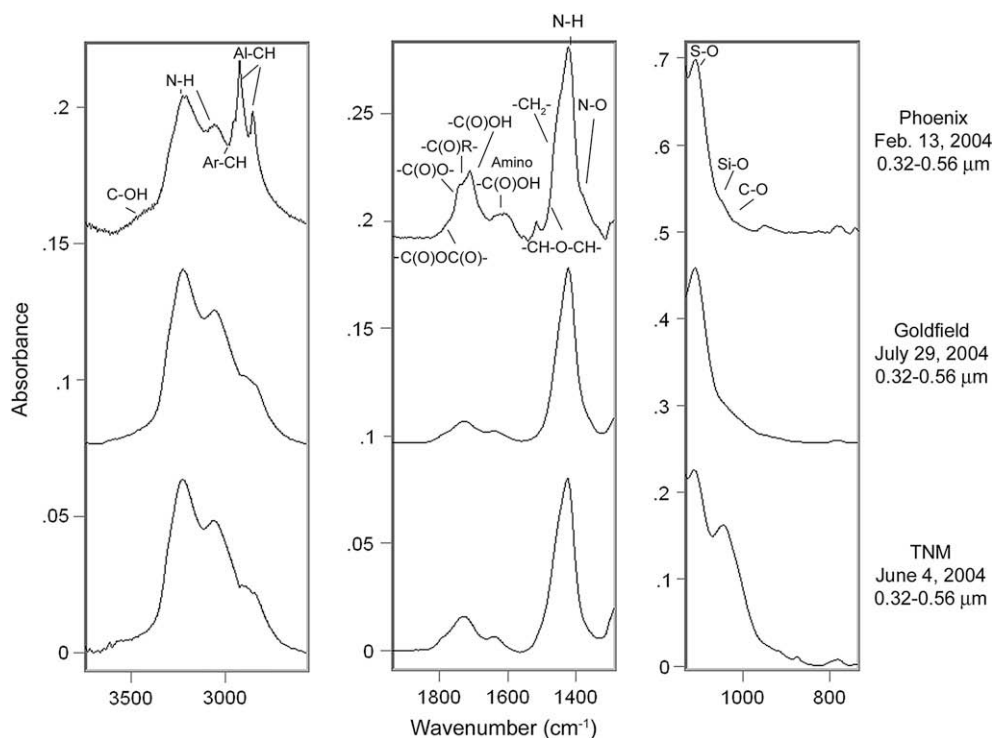

Fig. 2. Regions of IR spectra used in calibration for ambient spectra from samples collected in Phoenix, Goldfield and Tonto National Monument, AZ. Functional groups for each class of compounds listed in Table 1 are shown on the spectra from Phoenix. Aliphatic C–H (Al–CH) and aromatic C–H (Ar–CH) are abbreviated.

Table 1
Description of functional groups quantified.

Functional groups[a]	Atoms included in functional group
Methyl	$-CH_3$
Methylene	$-CH_2-$
Aliphatic	$-C-H$
Alkene	$-C=C-$
Aromatic	$-C-H$
Aldehydes/ketones	$-C(O)R-$
Carboxylic acids	$-C(O)OH$
Esters/lactones	$-C(O)O-$
Acid anhydrides	$-C(O)OC(O)-$
Carbohydrate ether	$-C-O-C-$
Carbohydrate hydroxyl	$-C-OH$
Amino acids	$-C(O)OH$
Amines	$-NH_2$
Ammonium nitrate	NH_4NO_3
Ammonium sulfate	$(NH_4)_2SO_4$

[a] Multiple compounds which contained each functional group were used in the calibration standards. A complete list of compounds used in the calibration can be found in the supplemental material of Coury and Dillner (2008).

functional group is the concentration of C(O)OH bonds found in all carboxylic acid molecules in the sample, not the concentration of carboxylic acid molecules. Although the C–O–C and C–OH functional groups in carbohydrates molecules are found in other organic compounds, the multivariate calibration which utilizing the entire spectrum not just one spectral region, minimizes misclassification of such functional groups. The matrix of functional group molar concentrations and the matrix of standard spectra were then entered into the PLS algorithm to generate the calibration. By using mixtures of compounds in each laboratory standard, multiple compounds were used to calibrate each functional group. For example, aliphatic mono- and dicarboxylic acids and aromatic poly-carboxylic acids were used to quantify the carboxylic acid functional group. The calibration was applied to the ATR-FTIR spectra of the ambient samples to determine the molar concentrations of functional groups. Mass concentrations ($ng\,m^{-3}$) were calculated from the predicted molar concentrations using the known molecular weight of the functional group. The sum of the mass of functional group and inorganic species measured by the ATR-FITR was on average 91% of parallel gravimetric mass measurements indicating that this method accurately measures absolute quantities of organic functional groups and inorganic ions (Coury and Dillner, 2008). The

following quantitative results are from the calibration. All measurements, including measurements below the minimum detection limits (MDL), as defined in Coury and Dillner (2008), are reported.

2.3. Trajectories

Twenty-four hour backward air trajectories were obtained for each sampling day at TNM. The trajectories were calculated with NOAA's HYSPLIT (Hybrid Single-Particle Lagrangian Integrated Trajectory) model version 4 using isentropic coordinates (Stohl, 1998) at a starting height of 500 m. This starting elevation was chosen because the terrain surrounding the Tonto National Monument sampling site is mountainous with heights above the sampling site of up to 500 m. Meteorological data from the National Weather Service's National Centers for Environmental Prediction (NCEP) gridded Meteorological Data Archives were used in HYSPLIT calculations. Each trajectory follows the probable path an air parcel traveled before arriving in TNM. Since each aerosol sample was collected over 24 h, twenty-four trajectories for each day (one air parcel path for each hour) were produced to determine where the air masses traveled prior to collection.

2.4. Statistical analyses

In order to compare the summer and winter ambient aerosol concentrations at TNM, probabilities were calculated using the non-parametric Mann–Whitney test. Probabilities less than 5% were considered statistically significant. Statistical analysis between seasons is only made for TNM because of the small data set for Phoenix.

In order to determine which functional groups and compounds were in the same air mass, the strengths of the linear relationships between functional group concentrations were determined by calculating the coefficient of determination, R^2.

3. Results and discussion
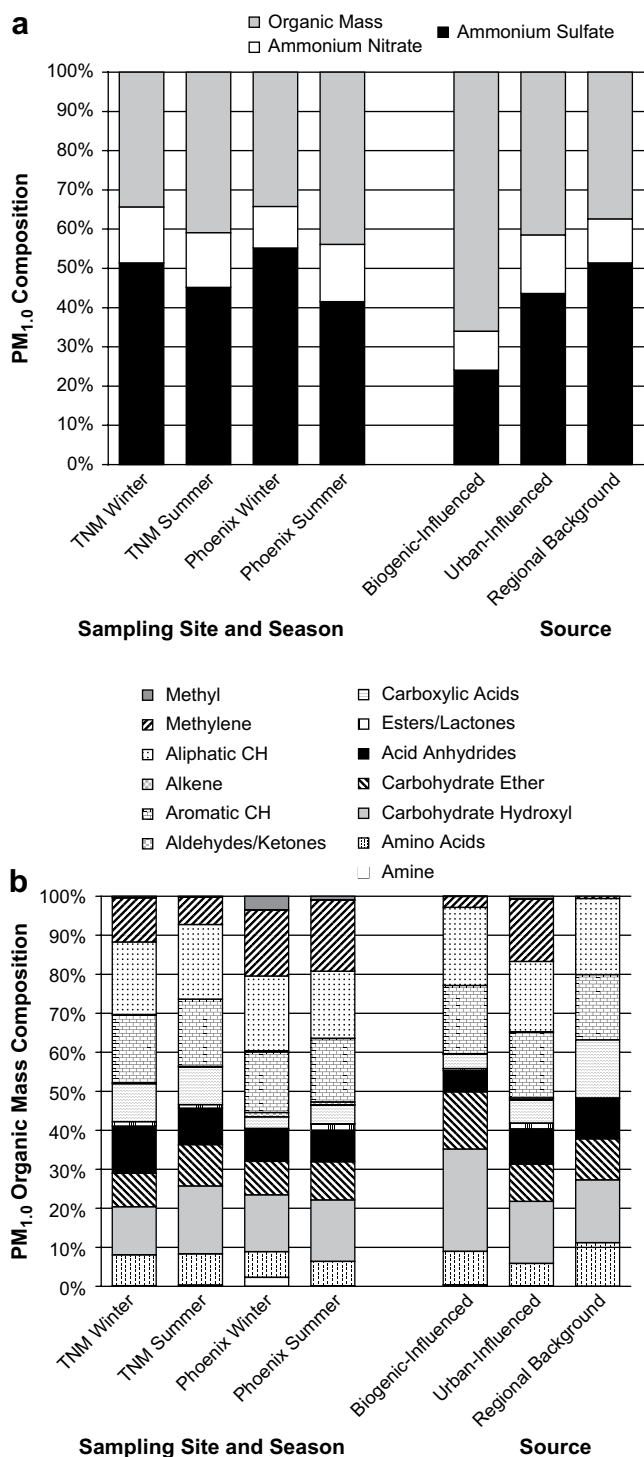
3.1. Composition of $PM_{1.0}$

FTIR-quantified $PM_{1.0}$ aerosol concentrations varied by sampling site and season; summer concentrations were higher than winter at

Table 2
Average concentrations ($ng\,m^{-3}$) of organic functional groups and inorganic ions by site and season and for source-influenced sampling events.

Functional group	Sampling site/season				Sources		
	TNM		Phoenix				
	Winter	Summer	Winter	Summer	Biogenic-influenced	Urban-influenced	Regional background
	$n^a = 8$	$n = 18$	$n = 2$	$n = 3$	$n = 1^b$	$n = 2$	$n = 3$
Methyl	4	5	28	15	2	11	0
Methylene	109	86	124	290	67	234	3
Aliphatic CH	137	200	120	289	478	263	82
Alkene	1	0	2	1	0	1	0
Aromatic	130	182	101	272	419	245	73
Aldehydes/ketones	3	2	9	12	3	7	0
Carboxylic acids	65	89	16	78	88	87	55
Esters/lactones	10	11	2	25	12	21	1
Acid anhydrides	86	93	46	131	130	132	41
Carbohydrate ether	63	114	54	167	350	139	46
Carbohydrate hydroxyl	95	190	96	273	628	232	72
Amino acids	50	80	37	106	205	85	45
Amines	1	3	13	1	8	0	0
Ammonium nitrate	319	361	193	551	356	523	124
Ammonium sulfate	1082	1096	1013	1569	873	1535	560

[a] Number of samples in the average.
[b] Dates of sampling events included in each source-influenced average concentration are given in Fig. 3.

a

b

Fig. 3. (a) Fractional composition of $PM_{1.0}$ determined by ATR-FTIR averaged by site and season (left) and averaged by source (right) (b) Fractional composition of $PM_{1.0}$ OM determined by ATR-FTIR averaged by site and season (left) and averaged by source (right). Atoms included in each functional group are listed in Table 1. The error bars are the aggregated uncertainties as defined in Coury and Dillner (2008). Biogenic-influenced data is from June 4, 2004. Urban-influenced data is the average of June 12 and 14, 2004 sampling days. Regional background data is the average of June 20, 26 and July 2, 2004 sampling days. The biogenic-influenced event has a high concentration of functional groups from carbohydrates and amino acids.

both sites (Table 2). Summer FTIR-quantified $PM_{1.0}$ concentrations (standard deviation) at TNM and Phoenix were 2.5 μg m^{-3} (0.93) and 3.8 μg m^{-3} (0.39), respectively. Winter $PM_{1.0}$ concentrations (standard deviation) at TNM and Phoenix were 2.2 μg m^{-3} (0.76) and 1.9 μg m^{-3} (0.65), respectively.

The FTIR-quantified $PM_{1.0}$ concentrations, averaged by site and season are in Table 2 and fractional compositions, averaged by site and season, are shown in Fig. 3. The FTIR-quantified $PM_{1.0}$ over the entire study consisted of ammonium sulfate (48%), ammonium nitrate (14%) and organic mass (OM) (38%). Ammonium sulfate concentrations were $\sim$1100 ng m^{-3} during summer and winter at TNM. However, ammonium sulfate was a statistically higher percentage of the $PM_{1.0}$ mass in the winter than in the summer and was over 50% of the mass in the winter at TNM (Fig. 3a). Ammonium nitrate $PM_{1.0}$ percent composition was $\sim$15% at TNM for both seasons. Organic mass concentrations averaged 1056 ng m^{-3} (41% of $PM_{1.0}$) at TNM during summer months, and 755 ng m^{-3} (34% of $PM_{1.0}$) during winter months. Percent composition at the two sites was similar (Fig. 3a). Ammonium sulfate, ammonium nitrate and OM concentrations were not statistically different by season at TNM.

3.2. Composition of organic aerosols

Concentrations of each functional group are given in Table 2 and the percent contributions of each functional group to the $PM_{1.0}$ OM quantified by FTIR are shown in Fig. 3b for both sampling sites averaged by season.

Aliphatic hydrocarbon functional group concentrations (aliphatic CH, methylene, methyl and alkene functional groups, see Table 1 for the atoms included in each functional group) contributed 30% and 26% of the organic mass at TNM in winter and summer respectively. Aromatic CH functional groups contributed about 16% of the organic mass for both sites and seasons (Fig. 3b). Aliphatic CH and methylene dominated the aliphatic hydrocarbon functional groups. Phoenix had much higher concentrations in the summer than winter and a higher percent of aliphatic hydrocarbons than TNM for both seasons. There were no statistical differences between summer and winter concentrations or % of OM for any aliphatic hydrocarbon or aromatic functional group at TNM. Maria and Russell (2005) measured aliphatic hydrocarbons (called alkanes) to be 69–81% of the $PM_{1.0}$ OM in summertime Princeton, NJ samples using the ambient peak in the IR spectrum at 2850–2920 cm^{-1} and quantified aromatic CH and found that it contributed 0–10% of the quantified OM. Although the FTIR methods are measuring similar functional groups, our site and method produce much lower OM percentages for aliphatic compounds. This is due in part to differences in the type of calibration (univariate vs. multivariate) used. Multivariate calibrations are better able to quantify functional groups which absorb in overlapping peaks, such N–H and C–H (for more information, see Coury and Dillner, 2008). Another cause for the difference between the Maria and Russell (2005) hydrocarbon measurements and this work are the number of organic functional groups quantified. Maria and Russell (2005) quantified seven organic functional groups that were included in the OM calculation, however, 13 functional groups (some the same and some different than Maria and Russell (2005)) were considered in this study which likely leads to a higher OM concentrations in our work. Using GC/MS analysis, Rogge et al. (1993) quantified over 80 organic compounds in ambient $PM_{2.1}$ aerosols at four urban sites in southern California. The compounds were converted into functional groups and aliphatic hydrocarbon functional groups (aliphatic CH, methylene, methyl and alkene) comprised between 50 and 55% of the sum of the annual average of quantified organic compounds and aromatic hydrocarbon functional groups comprised between 7 and 9% of the annual average of the quantified compounds. The aliphatic functional group % of OM in Rogge et al. (1993) was higher than measured in this study but lower than that measured by Maria and Russell (2005). The differences in the GC/MS functional group concentrations in Southern California and the ATR-FTIR functional group concentrations at TNM are in part

because highly polar compounds including esters and lactones, acid anhydrides and carbohydrates, which were measured by ATR-FTIR, were not measured in Rogge et al. (1993). Differences in the fraction of OM quantified, ~10% in Rogge et al. (1993) and ~90% in this work, add an additional uncertainty to the comparison.

Oxygenated functional groups, which include aldehyde/ ketone, carboxylic acid, ester/lactone, and acid anhydride functional groups (see Table 1 for atoms included in each functional group), contribute 23% and 20% of the organic mass at TNM for winter and summer as shown in Fig. 3b. The largest contributors were carboxylic acid functional groups (~10% of OM for both season) and acid anhydride functional groups (12% in winter and 10% in summer). Percentages of carboxylic acids and acid anhydrides at TNM were higher than Phoenix for both seasons. Aldehydes/ketones and esters/lactones were less than 2% for both sites and seasons and in contrast to carboxylic acids and acid anhydrides, aldehydes/ketones were lower at TNM for both seasons. Only acid anhydrides showed a statistical difference in percent of OM between seasons at TNM and were higher in the winter. Absolute concentrations showed no statistical difference for any oxygenated functional group at TNM. Carboxylic acid functional groups (from n-alkanoic acids, n-alkenoic acids, aliphatic dicarboxylic acids and aromatic polycarboxylic acids) comprised between 35 and 42% of the sum of the quantified organic compounds at the urban sites in Rogge et al. (1993). As with aliphatic hydrocarbons, the higher values obtained by Rogge et al. (1993) are due in part to GC/MS method not quantifying highly polar compounds. Rogge et al. (1993) quantified one aldehyde and several aromatic ketones and quinones which together had an average aldehyde/ketone functional group percent composition of 0.26% of quantified organic compound at all sites which compares to an overall average of 0.35% measured at TNM and Phoenix. Esters/lactones and acid anhydrides were not quantified in the Rogge et al. (1993) study and have not been quantified extensively elsewhere.

Biogenic functional groups (carbohydrate ether and hydroxyl, amino acids and amines, see Table 1 for the atoms included in each functional group) contributed on average 33% of the OM during the study period indicating that there was a considerable amount of biological material at both sites. Concentrations of carbohydrates and amino acids (Table 2) were statistically higher in summer than in winter at TNM. Carbohydrates as percent of OM were statistically higher in the summer (28%) than in the winter (21%) at TNM. These statistical differences are unchanged when sampling day June 4 which had very high biological functional group concentrations, is removed from the analysis. Nolte et al. (2001) quantified carbohydrates including levoglucosan and mono- and disaccharides in PM_3 at a background rural site and two urban sites in the San Joaquin Valley in California in winter by converting these highly polar compounds to their trimethylsilyl derivatives and analyzing by GC/MS. The concentration of carbohydrate ether and hydroxyl functional groups in the measured sugars was 144 ng m^{-3} at the background rural site (compared to winter concentrations at TNM of 158 ng m^{-3}) and an order of magnitude higher at the urban sites due to wood smoke. Another biogenic functional group, amino acids, made up 6–11% of the $PM_{1.0}$ organic mass and was not significantly different by season at TNM. The average amino acid functional group concentration, calculated from amino acid compounds measured in $PM_{2.5}$ collected in Davis, CA using high performance liquid chromatography (Zhang and Anastasio, 2003) was 117 ng m^{-3} and was estimated to be about 5% of the water soluble organic carbon. Amino acid functional groups were 50 and 80 ng m^{-3} for winter and summer at TNM and were 6–8% of the organic compounds in this study. This data suggests that the carbohydrate functional group and amino acid functional groups measured by the ATR-FTIR

method are comparable to those measured by other analytical techniques and are an appreciable fraction of organic particulate matter.

3.3. Sources of FTIR measured aerosol

Some functional groups may be present in the same molecule or come from the same source or source-type; this information may be ascertained by considering functional group correlations. Correlations were calculated between each functional group measured at TNM for one stage of the MOUDI, $D_a = 0.32$–0.56 μm, since this size bin has the largest fraction of data above MDL for most functional groups (Coury and Dillner, 2008). It is unlikely that the calibration method caused un-related functional groups to have high correlations because the concentration of each functional group was varied independently in the calibration standards (for example, carbohydrates were not always included with or varied in the same manner as the amino acids). Well correlated functional groups were put into groups and categorized as aliphatic CH and aromatic CH functional groups, saturated hydrocarbon functional groups, oxygenated functional groups, biogenic functional groups, and inorganic ions and are discussed in Section 3.3.1. Back trajectories and correlated functional groups concentrations were used to categorize sampling days into three source types: biogenic-influenced, urban-influenced and regional background, which are discussed in Sections 3.3.2–3.3.4.

3.3.1. Functional group correlations

Fig. 4 shows concentrations of correlated functional groups for each sampling date at TNM for $D_a = 0.32$–0.56 μm.

Aliphatic and aromatic CH are highly correlated ($R^2 = 0.997$). Methylene and methyl groups are highly correlated ($R^2 = 0.898$) and are classified as saturated hydrocarbon functional groups; however saturated functional groups are not highly correlated to the aliphatic and aromatic CH groups. Other groups discussed below are typically either correlated to the aliphatic and aromatic CH groups or the saturated groups but not both. Possible explanations for the correlations are given below. The alkene functional group had very low concentrations (Table 2) and is not highly correlated to any functional group measured so it is not included in Fig. 4.

Three of the four oxygenated functional groups, aldehydes/ ketones, esters/lactones and acid anhydrides are well correlated with each other ($R^2 > 0.868$). These groups are classified as oxygenated functional groups in Fig. 4. Anthropogenic and biogenic atmospheric organic material tends to become more oxygenated as it is transported in the atmosphere so these functional groups are expected to be correlated in part due to their secondary formation in the atmosphere (Jang and McDow, 1997; Blando and Turpin, 2000). They are also correlated with saturated hydrocarbons ($R^2 > 0.793$) which may be because these oxygenated functional groups are often attached to long carbon chains. The carboxylic acid functional group, which can be associated with straight chain or aromatic molecules, is both directly emitted and formed in the atmosphere from anthropogenic and biogenic precursors (for example, Blando and Turpin, 2000; Seinfeld and Pandis, 2006) and is not well correlated to any of the other measured oxygenated functional groups or any of hydrocarbon functional groups.

Carbohydrate ether and hydroxyl groups were highly correlated ($R^2 = 0.997$). The high correlation is expected because these functional groups are found in the same molecule. Amino acids correlate with carbohydrate ether ($R^2 = 0.880$) and hydroxyl ($R^2 = 0.870$) groups indicating that although amino acids and carbohydrates are two different types of molecules, they may be present in the same particle because they both come from biological sources. These functional groups are classified as biogenic functional groups in
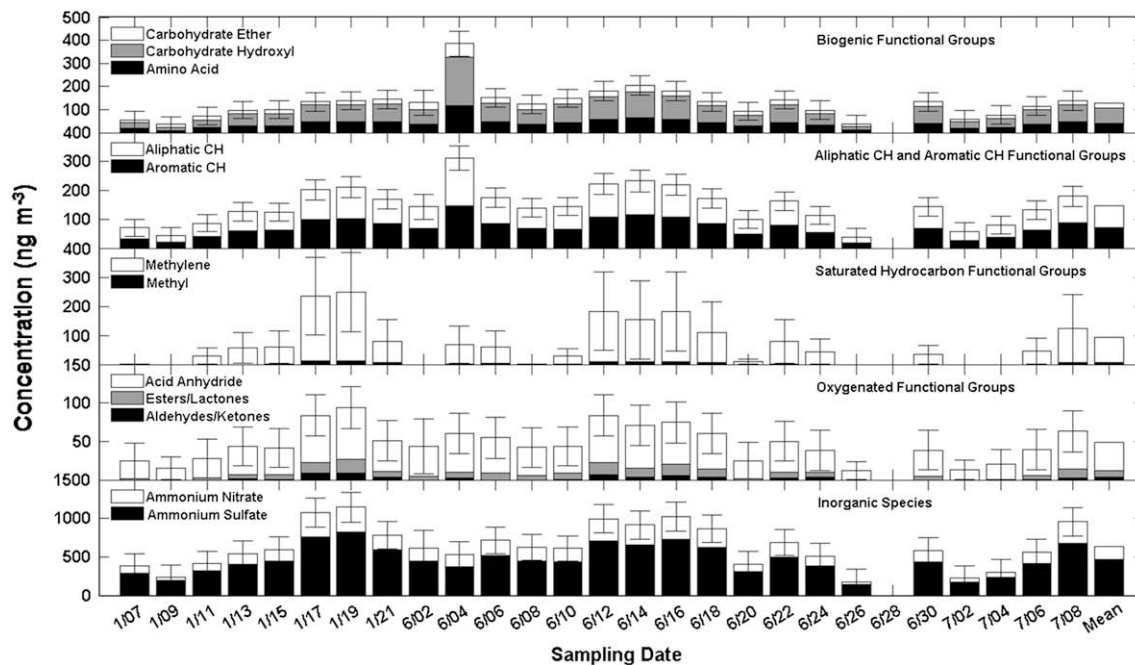
Fig. 4. Correlated functional group concentrations ($D_a = 0.32$–$0.56 \, \mu m$) at TNM for each sampling day with mean concentrations for sampling days shown at far right. Atoms included in each functional group are listed in Table 1.

Fig. 4. Amine concentrations were low and did not correlate with other functional groups. The carbohydrate functional groups also correlate well with aliphatic CH ($R^2 > 0.954$) and aromatic CH ($R^2 > 0.935$). Strong correlation with aliphatic CH is expected since carbohydrates are multifunctional compounds which contain multiple aliphatic CH functional groups. The large concentration of aliphatic CH observed in this work is likely due primarily to their presence in carbohydrate compounds.

Ammonium nitrate and sulfate are well correlated with $R^2 = 0.979$. Due to formation during transport, ammonium sulfate and ammonium nitrate are likely internally mixed particles. Other suspected secondary species, such as esters/lactones and acid anhydrides (Jang and McDow, 1997; Blando and Turpin, 2000; Hung et al., 2005), correlate well with ammonium sulfate and ammonium nitrate ($R^2 > 0.938$). Ammonium nitrate and ammonium sulfate are known anthropogenic secondary species, so a poor correlation with biogenic primary species was expected and observed.

Other size bins analyzed had very similar correlations when enough data was present. The following three sections characterize the three source groups using back trajectories, correlated functional group concentrations, and percent contributions of ions and organic functional groups to $PM_{1.0}$.

3.3.2. Primary biogenic-influenced sampling event

On June 4, 61% of the mass detected with ATR-FTIR analysis for $D_a = 0.32$–$0.56 \, \mu m$ was due to organic functional groups, higher than any other sampling day. The aerosol was characterized by high concentrations of biogenic functional groups; carbohydrate ether and hydroxyl, and amino acid concentrations were all approximately twice the mean value at TNM (see Fig. 4, last column for TNM means). Biogenic functional groups contributed 50% of the quantified $PM_{1.0}$ OM on June 4 (Fig. 3b) or nearly 1000 ng m^{-3} (Table 2) compared to 31% ($\sim$400 ng m^{-3}) on sampling days considered urban-influenced (see Section 3.3.3) and 38% ($\sim$100 ng m^{-3}) on sampling days considered to be regional background aerosols (see Section 3.3.4). Additionally, aliphatic CH and aromatic CH exhibited higher than mean

concentrations, whereas there were lower than mean concentrations of saturated hydrocarbons, inorganic species and most oxygenated functional groups. High concentrations of biogenic functional groups and aliphatic CH indicate that the particulate matter collected on this day consisted primarily of multifunctional highly branched or ringed carbohydrates. Carbohydrates are the most abundant biomolecules. Carbohydrates are found in the structure of plants (such as cellulose) and in wood smoke (such as levoglucosan) (Nolte et al., 2001). Components of vascular plant waxes such as phytosterols and triterpenoid acids, which contain carbohydrate hydroxyl groups and aliphatic CH groups, have been found in atmospheric aerosols (Nolte et al., 2002). Carbohydrate compounds such as sucrose and glucose have been found in soils (Gleixner et al., 2002; Simoneit et al., 2004a) and in ambient aerosols (Simoneit et al., 2004a,b). Proteins are another major class of biomolecules and are comprised of amino acids. They are found in plants and animals, and have also been found in soil due to the decomposition of proteinaceous material (Berthrong and Finzi, 2006) and in ambient aerosols (Zhang and Anastasio, 2003; Zhang et al., 2002).

In addition to the quantitative measurements showing high biogenic aerosols on June 4, qualitative inspection of the ambient IR spectra show high concentrations of silicate, a major component of soil. Fig. 5 shows the ambient spectrum (1300–900 cm^{-1}) for June 4 as well as the spectrum from June 20 for reference. Although silicate was not included in the FTIR calibration (see Coury and Dillner, 2008), it is apparent from these spectra that there were elevated concentrations of silicate on June 4 due to the unusually high Si–O peak at 1035 cm^{-1}.

The source of this aerosol is uncertain. High $PM_{1.0}$ biogenic and aromatic CH functional group loading suggests a forest fire but no fires were reported and a fire does not explain the high silicate loading. Road construction (including uprooting vegetation and clearing land from areas adjacent to the highway) was underway about 10 miles east-southeast of the sampling from 7am until the afternoon. Back trajectories show air masses passed over the general direction of the construction from 5:00am to 1:00pm. Although mechanical disturbances mostly produce particles larger
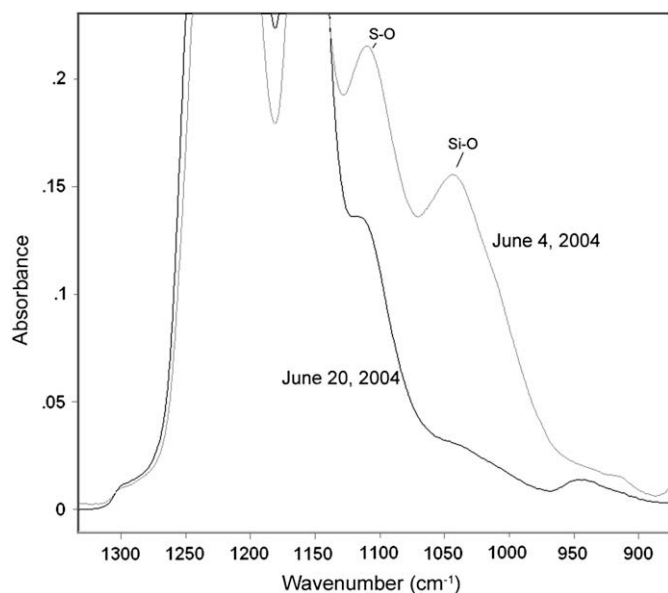
Fig. 5. IR spectra of ambient aerosols ($D_a = 0.32$–$0.56\ \mu m$) at TNM, June 4 and 20, 2004. June 4, 2004 is the biogenic-influenced sampling event.

than $PM_{1.0}$, it is possible that the construction activities contributed to the elevated biogenic and silicate aerosols and the heavy-duty diesel trucks used in the construction produced the high aromatic CH concentrations.

3.3.3. Urban-influenced aerosols

Aerosols at TNM influenced by urban sources arrive from Phoenix and are characterized by elevated concentrations of aliphatic and aromatic CH, saturated hydrocarbon, the correlated oxygenated functional groups and inorganic ions. June 12 and 14 back trajectories show direct, consistent flow over Phoenix and are the best examples of urban-influenced samples in this study. The average percentage above the mean concentration at TNM for these days, for the groups listed is 56% (Fig. 4). Other sampling days that are primarily urban-influenced (back trajectories show some flow through the Phoenix urban area, however they also show southern air flow from Mexico) are January 17, 19, June 2, 6, 8, 10, 16, 18 and July 8.

The total and organic masses ($D_a = 0.32$–$0.56\ \mu m$) on June 12 and 14 were the most compositionally similar to Phoenix samples and were likely a result of transport and photochemical reactions of emissions from Phoenix. Atmospheric lifetimes of some anthropogenic organic species (such as propene, m-xylene and acetaldehyde) which form secondary organic aerosols are 6–10 h (Seinfeld and Pandis, 2006) and trajectories show that air masses take on average 9 ± 7 h to reach TNM from Phoenix indicating that there is sufficient transport time for SOA to form. Phoenix samples were characterized by high percentages of saturated hydrocarbons (Fig. 3b) and high concentrations of all functional groups and inorganic ions (all were above 28% higher than TNM mean values). For methylene, June 12 and 14 had a higher concentration ($234\ ng\ m^{-3}$, Table 2) and percentage of OM (16%, Fig. 3b) than biogenic-influenced ($67\ ng\ m^{-3}$, 3%) and regional background ($3\ ng\ m^{-3}$, <1%) sampling days and their average concentrations were on average 82% higher than the mean (Fig. 4). N-alkanes, which can contain many methylene hydrocarbon functional groups, are a good indicator of "fresh" emissions (as demonstrated by their correlation to inert primary emissions of elemental carbon, (Rogge et al., 1993)). The correlated oxygenated functional groups were on average 57% higher than the TNM average (Fig. 4).

Ester/lactone concentrations were on average 72% above mean concentrations on June 12 and 14. Ester/lactone functional groups have been detected in secondary organic aerosol (SOA) in smog chamber experiments (Angove et al., 2006; Müller et al., 2008; Ziemann, 2005), and ambient aerosol particles (Mayol-Bracero et al., 2001). Acid anhydride concentrations were on average 55% higher than the mean concentration for June 12 and 14. Poly-aromatic hydrocarbon acid anhydrides have been detected in ambient aerosols (Allen et al., 1997) and as the oxidation product of a polycyclic aromatic hydrocarbon (PAH), benz[a]anthracene (Jang and McDow, 1997). Additionally, a pathway of anhydride formation from oleic acid ozonolysis was proposed by Zahardis et al. (2005). Thus, it is likely that the high concentrations of these oxygenated functional groups were due to secondary formation of particles from emissions from the Phoenix urban area. In addition, within the Phoenix urban area, heavy vehicular traffic is a known cause for high NO_x concentrations. Phoenix is the only major source of nitrate precursors within a hundred miles. Given transport times from Phoenix to TNM and the atmospheric lifetime of NO_2 of about 10 h (Seinfeld and Pandis, 2006), there is sufficient time for nitrate to form before reaching TNM. Therefore, the high concentrations (59% above mean for June 12 and 14, averaged) of ammonium nitrate on days when air parcels passed over the Phoenix area prior to arrival at TNM were not surprising. Ammonium nitrate also had the highest concentrations and percent contribution to $PM_{1.0}$ for the days considered urban ($523\ ng\ m^{-3}$, 15%) compared to biogenic ($356\ ng\ m^{-3}$, 10%) and regional background ($124\ ng\ m^{-3}$, 11%) sampling days (Table 2 and Fig. 3a, respectively).

3.3.4. Regional background aerosols

Regional background aerosols were characterized by lower than mean concentrations of inorganic ions and all organic carbon functional groups. Saturated hydrocarbons, aldehydes/ketones, and ester/lactone concentrations were often below the detection limits. Back trajectories were variable, mainly showing air flow from non-urban regions, however, some air arrived from the suburban areas of Phoenix. Sampling times with this signature were the first half of January and June 20 through July 4. June 20, 26, and July 2 trajectories did not travel over urban areas and are the best examples of regional background aerosols.

Quantified concentrations on June 20, 26, and July 2 were on average 58% below the mean for all functional groups and inorganic ions (Fig. 4). Saturated hydrocarbons not only had low concentrations (Table 2) but also were a low percentage of $PM_{1.0}$ organic mass (Fig. 3b). As stated above, n-alkanes, which can contain many saturated hydrocarbons, are typically a good indicator of "fresh" emissions (Rogge et al., 1993)). The lower percentages (or non-detection) of these groups indicate these sampling days (June 20, 26 and July 2) had low concentrations of primary emissions. Carboxylic acids and to a lesser extent acid anhydrides had higher % of OM during the regional background events than the urban or biogenic-influenced indicating higher relative concentrations of these secondary species. The regional background aerosols had higher percentage $PM_{1.0}$ concentrations (although the lowest concentration, Table 2) of the secondary species ammonium sulfate (51%, whereas urban days had 44% and biogenic days had 24%, Fig. 3a). Also, biogenic functional group concentrations were lower than for the other two source types (Table 2) and were a lower percentage of $PM_{1.0}$ OM (38%) than the biogenic sampling day (50%), but a higher percentage than urban sampling days (31%, Fig. 3b). The regional background aerosol has very low concentrations of all quantified groups, low percent contributions of primary emissions (either from Phoenix or biogenic influences) and high percent contribution from ammonium sulfate.

4. Conclusions

Size segregated aerosol samples were collected at a rural site downwind of the Phoenix in January, June and July of 2004. Size segregated samples were also collected at a site in downtown Phoenix and an urban fringe site, Goldfield, in February, July, and August of 2004. These samples were analyzed for organic and inorganic functional groups by ATR-FTIR spectroscopy using multivariate calibration techniques.

The mean percentage of $PM_{1.0}$ attributed to organic aerosol was 34% (14%) at TNM, with higher percentage in the summer than in the winter. Approximately 34% of the organic aerosol was composed of biogenic functional groups (carbohydrate ether, carbohydrate hydroxyl and amino acids). Carboxylic acids, which have been measured frequently in ambient aerosols and contribute a significant percentage of the measured organic compounds, and acid anhydrides, which have only been measured in a limited number of ambient samples and in small quantities, both contributed about 10% of the measured organic mass. Biogenic functional groups, showed a strong correlation to each other, indicating they are from the same source. Inorganic ions correlated well with each other due to similar formation pathways. Three of the four oxygenated functional groups also correlated well with each other likely because they are formed in the atmosphere.

During the sampling at TNM, three different air quality events were observed, which resulted in different $PM_{1.0}$ compositions. Sampling days were classified primary biogenic-influenced, urban-influenced, or regional background air quality events using the ambient concentration profiles, functional group correlations, and back trajectories. High concentrations of biogenic material were measured on June 4. Steady, direct air flow from the Phoenix urban area resulted in high concentrations of hydrocarbons, oxygenated functional groups, and inorganic species on June 12 and 14. Regional background aerosols, with very low concentrations of all quantified groups, occurred during half of the sampling days.

Appendix. Supplementary data

Supplementary data associated with this article can be found, in the online version, at doi:10.1016/j.atmosenv.2008.10.056.

References

Allen, J.O., Dookeran, N.M., Taghizadeh, K., Lafleur, A.L., Smith, K.A., Sarofim, A.F., 1997. Measurement of oxygenated polycyclic aromatic hydrocarbons associated with a size-segregated urban aerosol. Environmental Science & Technology 31, 2064–2070.

Angove, D.E., Fookes, C.J.R., Hynes, R.G., Walters, C.K., Azzi, M., 2006. The characterization of secondary organic aerosol formed during the photodecomposition of 1,3-butadiene in air containing nitric oxide. Atmospheric Environment 40, 4597–4607.

Berthrong, S.T., Finzi, A.C., 2006. Amino acid cycling in three cold-temperate forests of the northeastern USA. Soil Biology & Biochemistry 38, 861–869.

Blando, J.D., Porcja, R.J., Li, T.-H., Bowman, D., Lioy, P.J., Turpin, B.J., 1998. Secondary formation and the smoky mountain organic aerosol: an examination of aerosol polarity and functional group composition during SEAVS. Environmental Science & Technology 32, 602–613.

Blando, J., Turpin, B.J., 2000. Secondary organic aerosol formation in cloud and fog droplets: a literature evaluation of plausibility. Atmospheric Environment 34, 1623–1632.

Coury, C., Dillner, A.M., 2007. Trends and sources of particulate matter in the superstition wilderness using air trajectory and aerosol cluster analysis. Atmospheric Environment 41, 9309–9323.

Coury, C., Dillner, A.M., 2008. A method to quantify organic and inorganic compound classes in ambient aerosols using attenuated total reflectance FTIR spectroscopy and multivariate chemometric techniques. Atmospheric Environment 42, 5923–5932.

Gleixner, G., Poirier, N., Bol, R., Balesdent, J., 2002. Molecular dynamics of organic matter in a cultivated soil. Organic Geochemistry 33, 357–366.

Hung, H.M., Katrib, Y., Martin, S.T., 2005. Products and mechanisms of the reaction of oleic acid with ozone and nitrate radical. Journal of Physical Chemistry A 109 (20), 4517–4530.

Jacobson, M.C., Hansson, H.-C., Noone, K.J., Charlson, R.J., 2000. Organic atmospheric aerosols: review and state of the science. Reviews of Geophysics 38 (2), 267–294.

Jang, M., McDow, S.R., 1997. Products of Benz[a]anthracene photodegradation in the presence of known organic constituents of atmospheric aerosols. Environmental Science & Technology 31, 1046–1053.

Maria, S.F., Russell, L.M., Turpin, B., Porcja, R., Campos, T.L., Weber, R.J., Huebert, B., 2003. Source signatures of carbon monoxide and organic functional groups in Asian Pacific Regional Aerosol Characterization Experiment (ACE-Asia) submicron aerosol types. Journal of Geophysical Research 108 (D23), 8637.

Maria, S.F., Russell, L.M., 2005. Organic and inorganic aerosol below-cloud scavenging by suburban New Jersey precipitation. Environmental Science & Technology 39, 4793–4800.

Marple, V.A., Rubow, K.L., Behm, S.M., 1991. A Microorifice Uniform Deposit Impactor (MOUDI): description, calibration and use. Aerosol Science and Technology 14, 434–446.

Mayol-Bracero, O.L., Rosario, O., Corrigan, C.E., Morales, R., Torres, I., Perez, V., 2001. Chemical characterization of submicron organic aerosols in the tropical trade winds of the Caribbean using gas chromatography/mass spectroscopy. Atmospheric Environment 36, 1735–1745.

Mulik, J., Puckett, R., Williams, D., Sawicki, E., 1976. Ion chromatographic analysis of sulfate and nitrate in ambient aerosols. Analytical Letters 9, 653–663.

Müller, L., Reinnig, M.-C., Warnke, J., Hoffman, Th., 2008. Unambiguous identification of esters as oligomers in secondary organic aerosol formed from cyclohexene and cyclohexe/a-pinen ozonolysis. Atmospheric Chemistry and Physics 8, 1423–1433.

Nolte, C.G., Schauer, J.J., Cass, G.R., Simoneit, B.R.T., 2001. Highly polar organic compounds present in wood smoke and in the ambient aerosol. Environmental Science & Technology 35, 1912–1919.

Nolte, C.G., Schauer, J.J., Cass, G.R., Simoneit, B.R.T., 2002. Trimethylsilyl derivatives of organic compounds in source samples and in atmospheric fine particulate matter. Environmental Science & Technology 36, 4273–4281.

Pio, C.A., Alves, C.A., Duarte, A.C., 2001. Identification, abundance and origin of atmospheric particulate matter in a Portuguese rural area. Atmospheric Environment 35, 1365–1375.

Rogge, W.F., Mazurek, M.A., Hildemann, L.M., Cass, G.R., Simoneit, B.R.T., 1993. Quantification of urban organic aerosols at a molecular level: identification, abundance and seasonal variation. Atmospheric Environment 27A (8), 1309–1330.

Seinfeld, J.H., Pandis, S.N., 2006. Atmospheric Chemistry and Physics: from Air Pollution to Climate Change, second ed. John Wiley & Sons, Inc., New York.

Simoneit, B.R.T., Elias, V., Kobayashi, M., Kawamura, K., Rushdi, A.I., Medeiros, P.M., Rogge, W.F., Didyk, B.M., 2004a. Sugars-dominant water-soluble organic compounds in soils and characterization as tracers in atmospheric particulate matter. Environmental Science & Technology 38, 5939–5949.

Simoneit, B.R.T., Kobayashi, M., Mochida, M., Kawamura, K., Lee, M., Lim, H.-J., Turpin, B.J., Komazaki, Y., 2004b. Composition and major sources of organic compounds of atmospheric particulate matter sampled during the ACE-Asia campaign. Journal of Geophysical Research 109 (D19S10), 1–22.

Stohl, A., 1998. Computation, accuracy and applications of trajectories-A review and bibliography. Atmospheric Environment 32 (6), 947–966.

Yu, J., Flagan, R.C., Seinfeld, J.H., 1998. Identification of products containing –COOH, –OH, and –C=O in atmospheric oxidation of hydrocarbons. Environmental Science & Technology 32 (16), 2357–2370.

Zahardis, J., LaFranchi, B.W., Petrucci, G.A., 2005. Photoelectron resonance capture ionization-aerosol mass spectrometry of the ozonolysis products of oleic acid particles: direct measure of higher molecular weight oxygenates. Journal of Geophysical Research 110 (D08307), 1–10.

Ziemann, P.J., 2005. Aerosol products, mechanisms, and kinetics of heterogeneous reactions of ozone with oleic acid in pure and mixed particles. Faraday Discussions 130, 469–490.

Zhang, Q., Anastasio, C., 2003. Free and combined amino compounds in atmospheric fine particles ($PM_{2.5}$) and fog waters from Northern California. Atmospheric Environment 37, 2247–2258.

Zhang, Q., Anastasio, C., Jimenez-Cruz, M., 2002. Water-soluble organic nitrogen in atmospheric fine particles ($PM_{2.5}$) from northern California. Journal of Geophysical Research 107 (D11), 3-1–3-9.